Article

A Systematic Approach to Stable Grasping of a Two-Finger Robotic Hand Activated by Jamming of Granular Media

Osamah Fakhri [1] , George Youssef [2], Somer Nacy [1,2], Adnan Naji Jameel Al-Tamimi [3], O. Hussein [1], Wisam T. Abbood [1] , Oday Ibraheem Abdullah [4,5,6,]* and Nazar Kais AL-Karkhi [1]

1   Alkhwarzmi College of Engineering, University of Baghdad, Baghdad 10071, Iraq
2   Mechanical Engineering Department, San Diego State University, 5500 Campanile Drive, San Diego, CA 92182, USA
3   College of Technical Engineering, Al-Farahidi University, Baghdad 10001, Iraq
4   Energy Engineering Department, College of Engineering, University of Baghdad, Baghdad 10071, Iraq
5   Mechanical Engineering Department, College of Engineering, Gulf University, Sanad 26489, Bahrain
6   Institute of Laser and Systems Technologies (iLAS), Hamburg University of Technology (TUHH), Harburger Schloßstraße 28, 21079 Hamburg, Germany
*   Correspondence: oday.abdullah@tuhh.de

Abstract: A systematic approach is presented to achieve the stable grasping of objects through a two-finger robotic hand, in which each finger cavity was filled with granular media. The compaction of the latter, controlled by vacuum pressure, was used to adjust the structural and contact stiffness of the finger. The grasping stability was studied under the concurrent effect of an external torque and applied vacuum pressure. Stable grasping was defined as the no slippage condition between the grasped object and the two fingers. Three control schemes were adopted and applied experimentally to ensure the effectiveness of the grasping process. The results showed that stable and unstable grasping regions exist for each combination of applied torque and vacuum pressure. The two-finger robotic hands can be further improved for applications that require high load-carrying capabilities.

Keywords: jamming mechanism; granular media; stable grasping; variable stiffness

1. Introduction

The variety of tasks performed by artificial limbs necessitates a certain level of complexity that is embodied by their composition of several components, which must work together, synchronously or asynchronously, to achieve these tasks effectively. Like their natural counterparts, the upper artificial limb's hand (or end-effector) is of prime importance since it is responsible for executing numerous actions, including object grasping. The latter, however, appears trivial to humans and is a complicated action involving close coordination between the fingers to achieve safe and stable grasping. The fingers should grasp the object in a way that strikes a balance between avoiding excessive pressure, leading to breakage or deformation, and light pressure, leading to the slippage of the grasped object. Researchers have proposed and investigated several approaches to develop grasping mechanisms, where some considered the fingers as rigid components [1–3]. Others adopted flexible fingers, fingers with flexible surfaces as an interface for grasping, or fingers with flexible joints [4–10]. Moreover, under-actuated mechanisms have also been employed to achieve safe and stable grasping [11–18]. While these approaches have proved effective, the levels of control and accuracy are still far from the biomimicry of natural grasping.

A reexamination of natural grasping by the human hand indicates that this mechanism is dependent on the concept of the variable stiffness of each finger. In pursuit of the latter, roboticists recently emphasized the use of granular media in robotic grasping, in which the finger stiffness can be controlled and varied on demand during the grasping process. A novel, yet simple, way to achieve variable stiffness is the jamming of granular

media in a highly elastic sheath or a rubbery membrane, which was found to provide effectiveness in actuation [19] and stiffness tuning [20]. Robotic grippers [21,22], passive variable stiffness soft robotic grippers [23], articulated manipulators [24,25], the palm of a robotic hand [26], and the feet of mobile robots [27,28] are just a few prominent examples of integrating the jamming mechanism in practical applications. In grasping applications, the effectiveness of the jamming mechanism hinges on the symbiotic relationship between the two primary constituents, namely the granular media and the enclosing membrane. The process of jamming of the granular media, i.e., the reversible relative motion of the particles, was demonstrated using a hydraulic or pneumatic control system [29–32], and pneumatic muscles in soft grippers [33]. The membrane plays a starring role beyond the elastic confinement of the particles, including stiction, flexibility, and a high degree of reversibility [34,35]. The shape, size, and morphology of grains are effective in the performance of granular grippers [36,37].

Despite the startling advancements reported in recent years in grasping through jamming, there is a need for a holistic and systematic approach to developing and controlling variable-stiffness fingers that closely resemble their natural counterparts. The objective of this research was to develop a two-finger hand based on the jamming of granular media, where the membrane of each elastic finger was filled with particles and was operated by varying the vacuum pressure. This vacuum pressure was developed using a vacuum pump, and maintained and monitored using a solinod valve and a pressure gauge. The grasping force was estimated not only by the externally applied torque of the servomotor but also by defining a relationship between the finger stiffness and the vacuum pressure. A feedback control system was developed and implemented to track the signal indicating slippage initiation between the finger and the grasped object, observed by a linear variable differential transformer. At this point, the servomotor torque and each finger stiffness are varied to suppress the sliding or slippage of the grasped object. The control system consists mainly of an Arduino board and a PC.

2. Stiffness Analysis and Measurements

The finger stiffness plays the primary role in defining grasping effectiveness based on the interplay between the kinematics of the finger and the intricate motion of the granular media upon vacuum application. Based on the given dynamic interactions between the former and the latter, an experimental approach was employed to determine and analyze the stiffness of the finger. In doing so, the finger was assumed to be a cantilever beam, as shown schematically in Figure 1, where the finger stiffness is defined based on the contribution of the deflection of the cantilever finger (w) and the deformation of the surface of the finger (δ). Both deformations are due to the applied force (F). The former deformation is related to the force applied through the beam's structural stiffness ($k_b = F/w$) while the latter is associated with the beam surface contact stiffness ($k_s = F/\delta$). It is important to note that finger stiffness depends not only on the geometry but also on the material properties. The finger's mechanical properties mainly depend on the vacuum pressure subjected to the granular media inside the finger cavity, found experimentally as discussed below. Therefore, the overall finger stiffness can be calculated based on Equation (1).
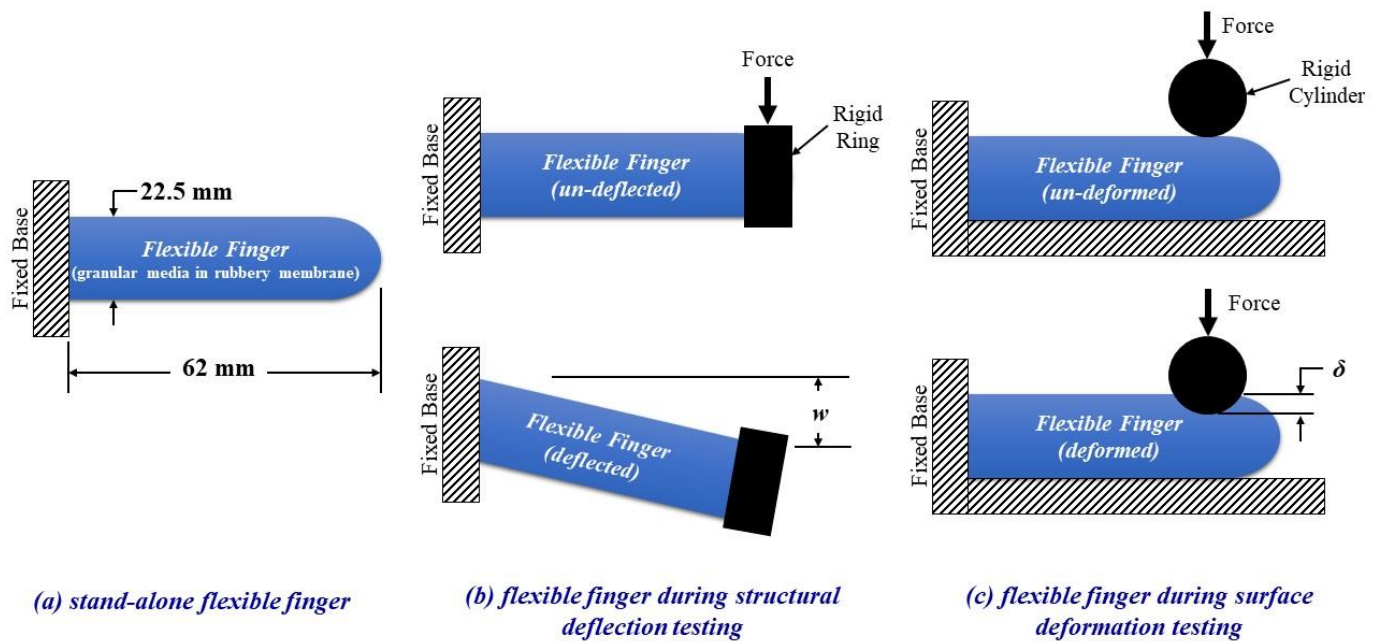
(a) stand-alone flexible finger

(b) flexible finger during structural deflection testing

(c) flexible finger during surface deformation testing

Figure 1. (**a**) Geometric configuration of flexible finger with granular media and elastic membrane, (**b**) representation of the structural testing to find the force–deflection data, and (**c**) surface contact testing to report force–deformation behavior.

$$k_t = \frac{k_s k_b}{k_b + k_s} \tag{1}$$

where:

k_t is the overall stiffness of the finger;

k_s is the surface contact stiffness;

k_b is the structural stiffness.

A physical artificial finger was made by filling a compliant elastic membrane with spherical particles made of resin beads with a density of 0.37 g/cm^3 and a nominal diameter of 1.75 mm. The nominal diameter and length of the finger were 22.5 mm and 62 mm, respectively. The grasped object considered in this study was a rigid cylinder with a 25 mm diameter, 80 mm length, and a mass of 61 g. Tests were conducted using a universal tensile testing machine, which was used to apply a controlled force to obtain both the structural and surface contact stiffness of the finger. A rigid ring was fixed at the free end of the finger, as clarified in Figure 1b, to ensure that the force (F) would induce the deflection (w) only, with no effect on the surface contact deformation. All measurements were carried out under different vacuum pressures ranging between 0 and 0.5 bar at different applied loads. Each test was repeated five times, and the average is considered in the results. Figure 1a shows a schematic of the artificial finger with dimension and boundary conditions, Figure 1b demonstrates the experimental setup to measure the structural stiffness, and Figure 1c represents the protocol followed for obtaining the surface contact stiffness.

3. Experimentation and Procedure

Following the characterization of the stiffness of individual fingers, a two-finger robotic hand was designed and fabricated, as shown in Figure 2, where the jamming of the granular media was controlled using a vacuum pump (Kamoer HLVP15-AU24). At the same time, the pressure was measured using a pressure gauge and maintained using a solenoid valve (generate Model 2W-025-08). The two-finger hand was moved horizontally by a geared platform powered by a servomotor (PFN-13ED04D) to control the gripping functionality. Before starting a test, the fingers were checked to ensure a leakage-free state by monitoring the pressure gauge reading. According to the type of

signals transferred in the system during operation, the system can be divided into three subsystems: mechanical, pneumatic, and measurement and control, as demonstrated by the block diagram in Figure 2. The mechanical subsystem consists of the load and torque applied to the fingers and grasped object, respectively. The pneumatic subsystem applies and maintains the vacuum pressure inside the elastic fingers. Finally, the measurement and control of the displacement of the grasped object is achieved through the measurement and control subsystem. The demonstration of the operation was performed in two steps. The two-finger hand's load-carrying capacity was estimated at different servomotor-applied torques and different vacuum pressures. The latter was varied between 0 and 0.5 bar, while the former was changed from 1.16 N-m to 1.42 N-m, where, according to the instruments' specifications, the maximum allowable applied torque and vacuum pressure were 1.42 N-m and 0.5 bar, respectively. Figure 2a shows the mechanism used to estimate the load-carrying capacity. At each combination of vacuum pressure and torque, an axial load was applied through the linear actuator (LA-M-12-40-30-50/105) attached to the grasped object until the object started to slide away from the fingers. A linear variable differential transformer (EVAL-CFTL-LVDT-ND) recorded the sliding action. The load corresponding to the onset of sliding was considered the critical load, above which grasping stability is lost.
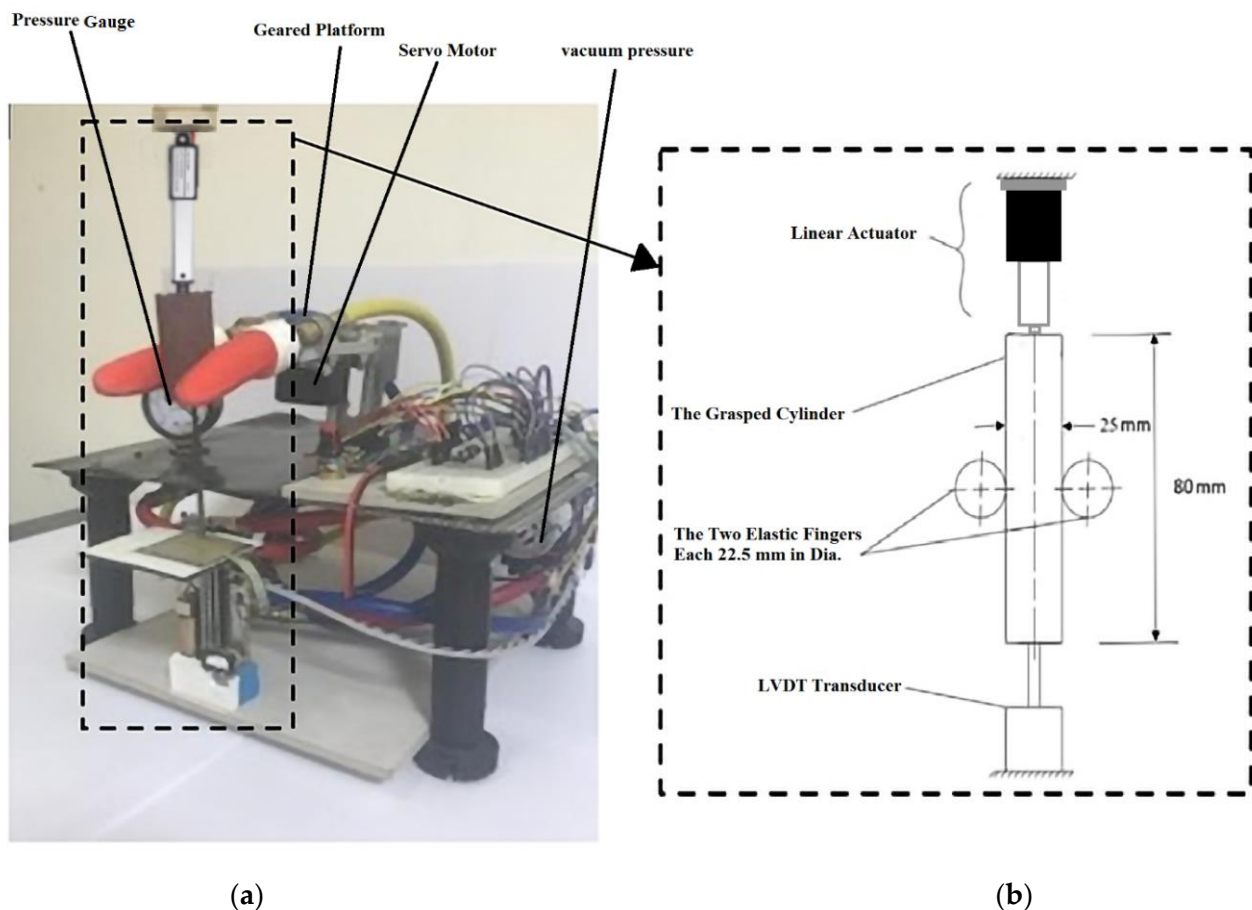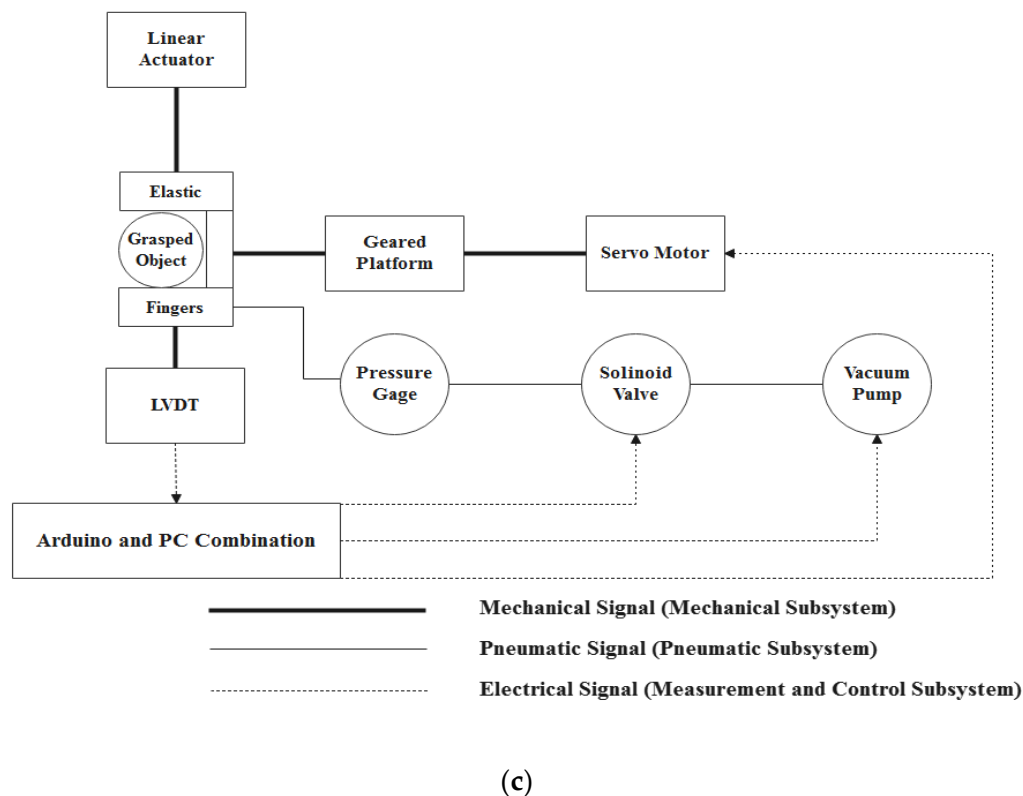

(**a**)　　　　　　　　　　　　　　　　　　　　(**b**)

Figure 2. *Cont.*

(c)

Figure 2. (**a**) The two-finger robotic hand. (**b**) Schematic of the load-carrying mechanism. (**c**) Block diagram of the system.

Second, the performance and control of the two-finger robotic hand were investigated and characterized. An axial load was applied to the grasped object as a step input until slippage started. Concurrently, the mechanism adopted was prohibited from sliding by varying the applied torque and the vacuum pressure using one of three different control procedures (Figure 3). The Arduino board was programmed according to the algorithm of each procedure (i.e., the individual flowcharts in Figure 3). Regardless of the control procedure, the input signal was the load applied on the grasped object, while the output signal was the sliding motion sensed by the displacement transducer. The LVDT signal was also considered a feedback signal for the servomotor and the vacuum pump to adjust the grasping force to prevent sliding. At the initiation of sliding, and according to the first procedure, Figure 3a, the servomotor was activated by the feedback signal; hence, the applied torque started to increase until sliding stopped. If sliding persisted until the maximum allowable torque was reached, then the vacuum pump was activated to reach stable grasping, i.e., no sliding. In the second procedure, Figure 3b, the vacuum pump was first activated according to the feedback signal. The vacuum pressure started to increase to suppress sliding. If sliding continued until the maximum allowable vacuum pressure was attained, then the grasping force was increased by activating the servomotor until a stable grasping condition was approached. In the above two procedures, the activation of either the servomotor or the vacuum pump was conducted sequentially, or, as one stopped, the other started. In the third procedure, as described in the flowchart in Figure 3c, the servomotor and the vacuum pump were concurrently activated after receiving the feedback signal from the controller. In the third control procedure, both the applied torque and vacuum pressure were increased simultaneously until the stable grasping condition was reached. It is clear that the adoption of the above three procedures is due to the main factors affecting grasping, namely the vacuum pressure and the servomotor torque. Each one was varied separately in the first two procedures, while in the third procedure, both factors varied simultaneously.
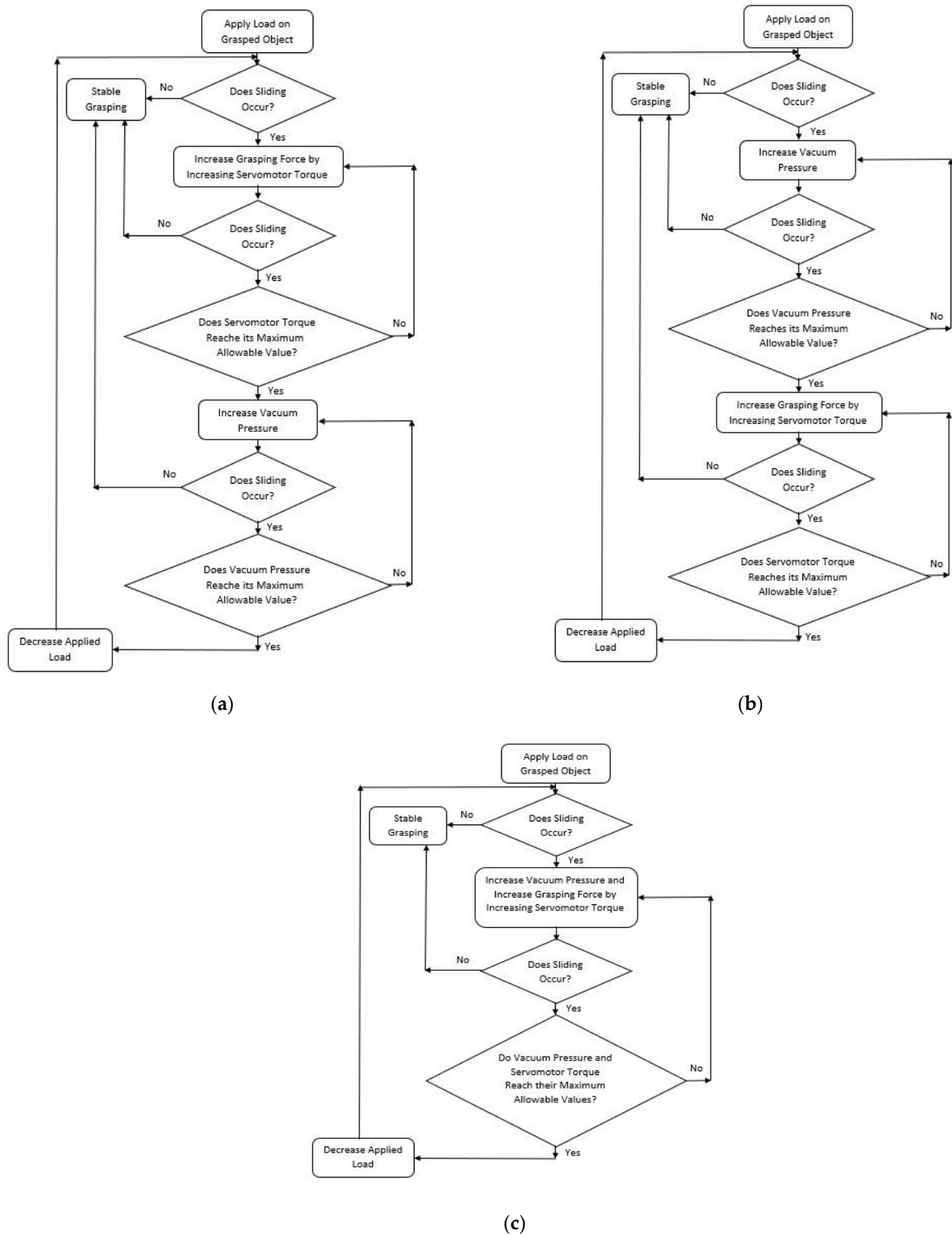
(**a**)

(**b**)

(**c**)

Figure 3. Flowcharts of the three control procedures. (**a**) The servomotor was activated by the feedback signal. (**b**) The vacuum pump was first activated according to the feedback signal. (**c**) The servomotor and the vacuum pump were concurrently activated after receiving the feedback signal from the controller.

4. Results and Discussion

One of the main promising advantages of the investigated flexible fingers is the ability to tune or vary the stiffness on demand throughout the grasping process. Hence, flexible fingers can potentially grasp different objects with various shapes without deforming or crushing these objects. The flexible finger's overall variable stiffness comprises two components, namely bending or structural stiffness and surface contact stiffness, as discussed before. The relationships between the applied load and the resulting deflections (bending and surface) are shown in Figure 4. For the case of bending stiffness, Figure 4a shows the linear relationship between load and deflection regardless of the vacuum pressure used in the jamming process of the granular media within the finger cavity, where the elastic finger behaves as a cantilever beam. This monotonic relationship implies that stiffness has a constant value of 0.75, 1.25, 1.82, 2.07, and 2.67 N/m for vacuum pressures of 0, 0.2, 0.3, 0.4, and 0.5 bar, respectively. On the other hand, Figure 4b reports the nonlinear relationship between load and deflection for the surface contact loading due to the Hertzian contact behavior between the solid grasped object and the elastic finger. The results in Figure 4b signify the ability to tune the contact stiffness, i.e., grasping effectiveness, as a function of the applied load and vacuum pressure, where the slope of the force–deflection curve is the tangent contact stiffness. Interestingly, the contact stiffness at maximum load was found to be nearly constant at a value of 48.5 N/mm at the highest vacuum pressure used in this experiment (0.5 bar). The plateau of the contact stiffness at a high load and vacuum pressure is attributed to the saturation of the jamming process, where the application of an additional vacuum does not yield any noticeable increase in the compaction of the granular media.

Furthermore, due to the maximum compaction, the finger surface does not exhibit any additional indentation as the load incrementally increases. Therefore, it is important to note that the jamming process, due to an increasing vacuum pressure effectively tunes both the bending and surface contact mechanisms such that both stiffnesses correspond to an increase in vacuum pressure. The overall stiffness of the flexible finger with respect to the vacuum pressure is presented in Figure 4c, demonstrating a quasi-linear relationship between the overall stiffness and vacuum pressure. Overall, the ability to concurrently tune the bending and contact stiffness indicates the technological potential of the flexible finger in gripping and grasping applications.

The load-carrying capacity of the two-finger hand is governed mainly by the vacuum pressure in each finger and the externally applied torque of the servomotor, which induces the normal force at the interface between each finger and the grasped object. The results show that increasing the applied torque and the vacuum pressure enhances the load-carrying capacity, as shown in Figure 5. The rate of the carried load increased as the vacuum pressure increased, which is attributed to the increase in the stiffness of each finger. Therefore, the applied torque provides the ability to grasp the object without deforming the finger due to contact between the finger and the grasped object. The stable grasping region of the investigated flexible fingers for each applied torque is located below the curve relating the load-carrying capacity with the vacuum pressure, at which point there is no slippage between the fingers and the grasped object. It is imperative to realize that the grasping effectiveness, shown as load-carrying capacity, is based on the geometrical and material attributes used to fabricate the flexible fingers. Nonetheless, further tailoring of the finger performance can be accomplished by changing the geometry of the finger (nominal diameter and length) and the attributes of the granular material (nominal particle size, particle material, compaction volume, etc.). The systematic approach reported herein can then be used to comprehensively characterize and stably control the two-finger hand.
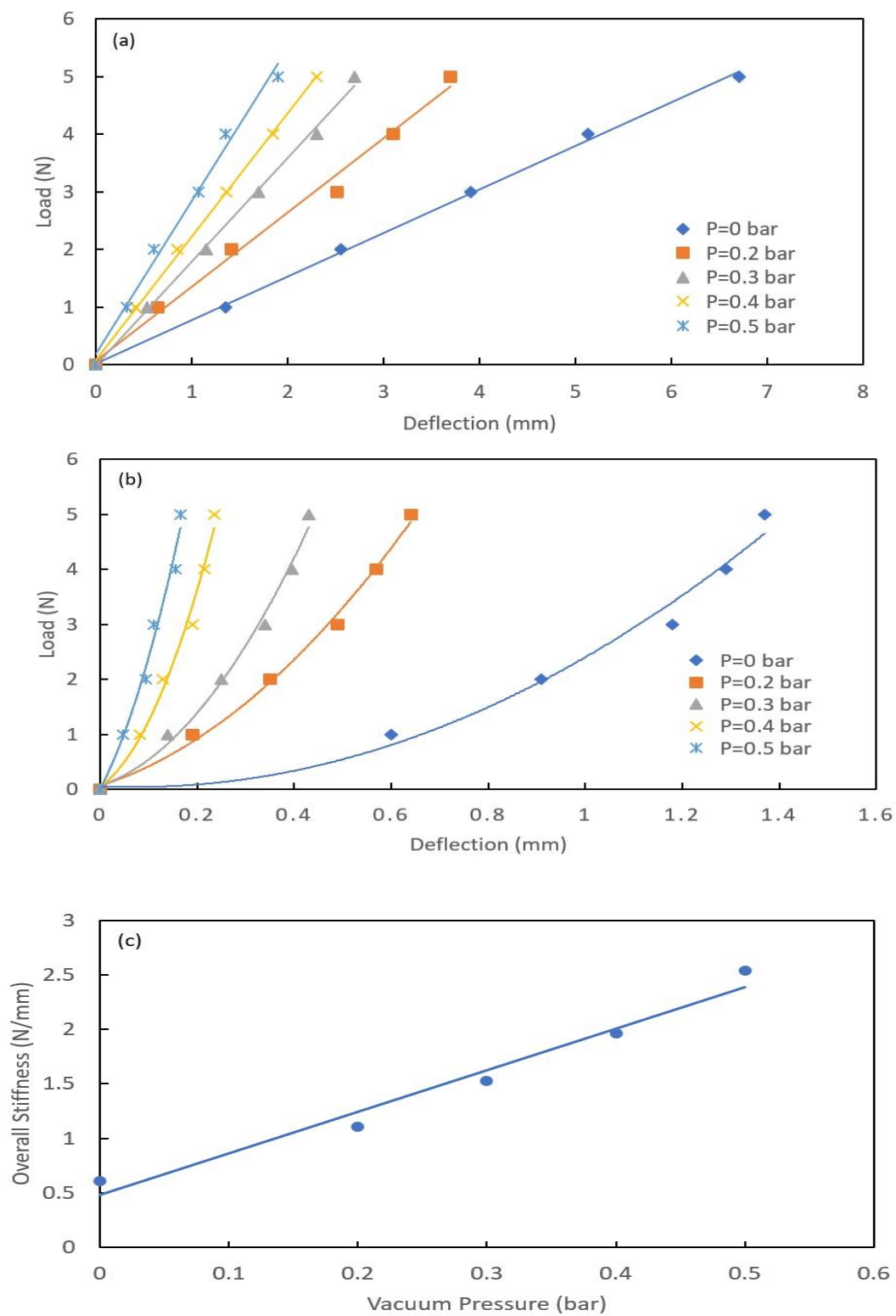
Figure 4. (**a**) Structural load–deflection characteristics of the elastic finger. (**b**) Surface contact load–deflection characteristics of the elastic finger. (**c**) The overall stiffness variation with vacuum pressure.
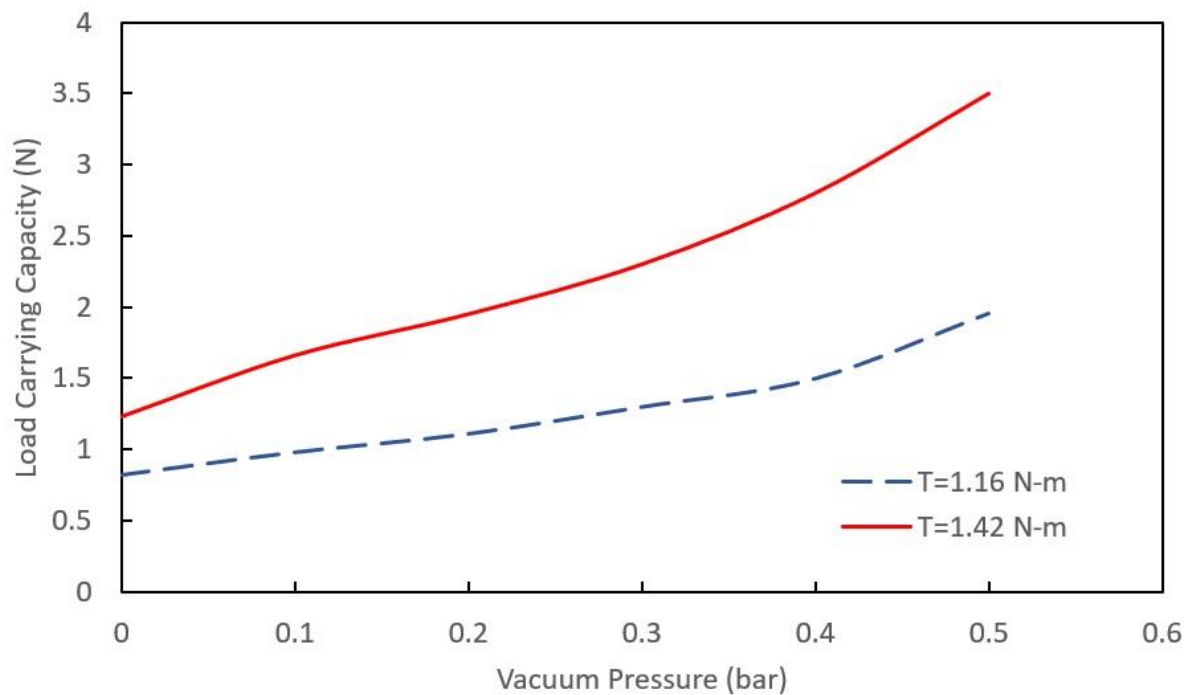
Figure 5. The load-carrying capacity of the two-finger hand as a function of vacuum pressure and applied torque, where the area under each curve constitutes the condition of stable grasping for this specific torque.

The dynamic performance of the two-finger hand was investigated and controlled using the three procedures stated previously. Three different loads (1.5, 2.5, and 3.5 N) were applied to the grasped object stepwise for each procedure. Three metrics were used to assess the effectiveness of each procedure:

- The occurrence of stable grasping or not;
- The sliding distance traveled by the grasped object until the stable grasping condition was reached;
- The time required to reach stable grasping condition.

The dynamic response of the two-finger hand for the first loading case (i.e., 1.5 N) using the three control procedures is presented in Figure 6a. The fastest response to attain a stable grasping condition was achieved by the third procedure within 48 ms, followed by the first procedure within 59 ms, and the slowest response is from the second procedure within 110 ms. However, the sliding distance of the grasped object to stable grasping is less for the third procedure, as compared to the other two procedures. The displacement–time histories based on the first and third procedures when the load increased to 2.5 N are shown in Figure 6b. The time to achieve stable grasping was found to be 150 ms and 70 ms, respectively. In the case of 2.5 N, stable grasping was not attained using the second control procedure. Finally, for a load of 3.5 N, the third procedure was the only schema able to achieve stable grasping within 120 ms, as shown in Figure 6c. Therefore, the most effective procedure to reach stable grasping is the third procedure, whereas the first and second procedures fail to attain a stable grasping condition as the load carried by the grasped object increases.
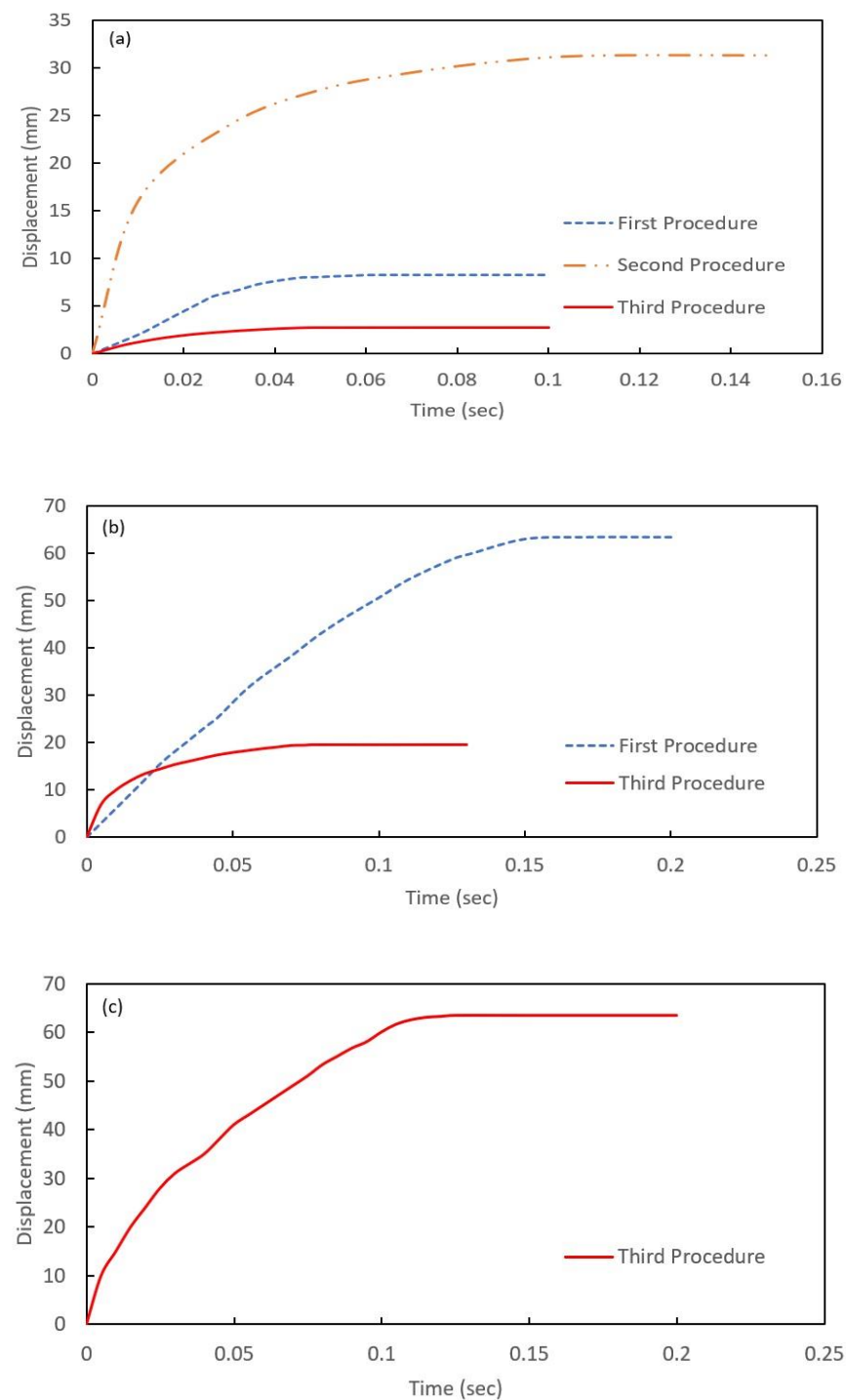
Figure 6. The dynamic response of the flexible two-finger hand with an applied load of (**a**) 1.5 N, (**b**) 2.5 N, and (**c**) 3.5 N, showing control procedures that were able to achieve stable grasping.

The dichotomy between the transient response of the vacuum-assisted jamming process and the torque applied by the servomotor is the prime decider of the success of a control procedure as a function of the applied load. In other words, the combined effects of the servomotor torque and vacuum pressure lead to the stable grasping condition, where the induced grasping force depends on the vacuum pressure inside the finger cavity for a specific servomotor torque applied. However, the timing difference in applying the torque and pulling the vacuum is inherently crucial, given the dynamic nature of the investigated grasping process. For example, it was found that the time required for the servomotor to

reach its maximum torque supply of 1.42 N-m was 45 ms, while the vacuum pump took 150 ms to reach a maximum pressure of 0.5 bar in the fingers' cavities. It is important to note that these are limitations of the constructed experimental setup and can be improved by adopting different servomotors and vacuum pumps; the hardware evaluation was beyond the scope of the current research. Hence, the second procedure could not attain a stable grasping condition for two of the loads applied to the grasped object. In the second control schema, the vacuum pump was first activated due to the time needed to reach maximum vacuum pressure being longer than the time required to apply maximum torque. Subsequently, the load was incrementally applied to the grasped object, resulting in slippage before reaching force equilibrium. That is, the lag between attaining vacuum pressure and applied torque resulted in unstable grasping. In contrast, the third procedure was able to sustain loads up to 3.5 N, or, in other words, attain stable grasping even when relatively high loads were applied to the object. Collectively, this points towards the ability of the investigated novel two-finger robotic hand to stably grasp cylindrical objects without crushing them while adjusting grasping force on demand. Future research will focus on investigating the effect of the nominal diameter of the granular media as well as the quality of the hardware on achieving effective grasping at higher loads applied to numerous other grasped object geometries.

5. Conclusions

This research investigated a novel approach to grasping based on the jamming of granular media packed within an elastic membrane using vacuum pressure. A two-finger robotic hand was designed, tested, and controlled to achieve stable grasping without slippage by leveraging each finger's structural and contact stiffness. It was found that finger stiffness has a dominant effect on attaining a stable grasping condition. This stiffness was found to increase almost linearly with increasing vacuum pressure. In order to extend the applicability of the current two-finger hand, the load-carrying capacity to attain a stable grasping condition was also investigated, which was accomplished using three different control procedures. It was found that the maximum load-carrying capacity was 3.5 N and 1.8 N for applied torques of 1.42 N-m and 1.16 N-m, respectively.

Each of the control procedures alternated the sequence of applying the vacuum pressure and the applied grasping force on each finger. When the vacuum pump and the applied torque were applied concurrently, i.e., in the third procedure, the highest load-carrying capacity was achieved, as compared to the other two procedures. The relatively low load-carrying capacity reported herein was associated with the limitations imposed by the specifications of the components used in this mechanism rather than the approach to achieve stable grasping. In other words, jamming granular media using vacuum pressure while concurrently applying a gripping force can stabilize grasping even in high load-carrying applications. The latter can be achieved by using different hardware components with higher operational characteristics. Overall, the outcomes of this research indicate a successful control scheme to attain stable grasping conditions through the variable flexibility of a two-finger hand without crushing or breaking the grasped object.

References

1. Yussof, H.; Ohka, M. Grasping Strategy and Control Algorithm of Two Robotic Fingers Equipped with Optical Three-Axis Tactile Sensors. *Procedia Eng.* **2012**, *41*, 1573–1579. [CrossRef]
2. Nacy, S.; Tawfik, M.; Baqer, I. A Novel Fingertip Design for Slip Detection Under Dynamic Load Condition. *ASME J. Mech. Robot.* **2014**, *6*, 031009. [CrossRef]
3. Nacy, S.; Tawfik, M.; Baqer, I. A Novel Approach to Control the Robotic Hand Grasping Process by Using an Artificial Neural Network Algorithm. *J. Intell. Syst.* **2017**, *26*, 215–231. [CrossRef]
4. Khurshid, A.; Khan, Z.; Chacko, V.; Ghafoor, A.; Malik, M.; Ayaz, Y. Modelling and Simulation of a Manipulator with Stable Viscoelastic Grasping Incorporating Friction. *Tribol. Ind.* **2016**, *38*, 4.
5. Alspach, A.; Kim, J.; Yamane, K. Design and Fabrication of a Soft Robotic Hand and Arm System. In Proceedings of the IEEE International Conference on Soft Robotics (RoboSoft), Livorno, Italy, 24–28 April 2018.
6. Garate, V.; Pozzi, M.; Prattichizzo, D.; Ajoudani, A. A Bio-inspired Grasp Stifness Control for Robotic Hands. *Front. Robot. AI* **2018**, *5*, 89. [CrossRef]
7. Vedhagiri, G.; Prituja, A.; Li, C.; Zhu, G.; Thakor, N.; Ren, H. Pinch Grasp and Suction for Delicate Object Manipulations Using Modular Anthropomorphic Robotic Gripper with Soft Layer Enhancements. *Robotics* **2019**, *8*, 67. [CrossRef]
8. Yamaguchi, T.; Kashiwagi, T.; Arie, T.; Akita, S.; Takei, K. Human-Like Electronic Skin-Integrated Soft Robotic Hand. *Adv. Intell. Syst.* **2019**, *1*, 2. [CrossRef]
9. Simone, F.; Rizzello, G.; Seelecke, S.; Motzki, P. A Soft Five-Fingered Hand Actuated by Shape Memory Alloy Wires: Design, Manufacturing and Evaluation. *Front. Robot. AI* **2020**, *7*, 608841. [CrossRef]
10. Ruotolo, W.; Brouwer, D.; Cutkosky, M.R. From Grasping to Manipulation with Gecko-Inspired Adhesives on a Multi-Finger Gripper. *Sci. Robot.* **2021**, *6*, eabi9773. [CrossRef]
11. Spanjer, S.; Balasubramanian, R.; Herder, J.; Dollar, A. Improved Grasp Robustness through Variable Transmission Ratios in Underactuated Fingers. In Proceedings of the IEEE/RSJ International Conference on Intelligent Robots and Systems, Vilamoura-Algarve, Portugal, 7–12 October 2012.
12. Rojas, N.; Ma, R.; Dollar, A. The GR2 Gripper: An Underactuated Hand for Open-Loop In-Hand Planar Manipulation. *IEEE Trans. Robot.* **2016**, *32*, 763–770. [CrossRef]
13. Nacy, S.; Nayif, A. Simulation Analysis of Grasping Forces for a 3-DOF Robotic Manipulator. *Innov. Syst. Des. Eng.* **2016**, *7*, 11.
14. Ha, X.; Ha, C.; Nguyen, D. A General Contact Force Analysis of an Under-actuated Finger in Robotic Hand Grasping. *Int. J. Adv. Robot. Syst.* **2016**, *13*, 14. [CrossRef]
15. Li, X.; Huang, Q.; Chen, X.; Yu, Z.; Zhu, J.; Han, J. A Novel Under-actuated Bionic Hand and its Grasping Stability Analysis. *Adv. Mech. Eng.* **2017**, *9*, 2. [CrossRef]
16. Nacy, S.; Nayif, A. Effect of Object Size and Location on Contact Forces and Grasping Stability for an Underactuated Robotic Manipulator. *J. Mechatron. Robot.* **2018**, *2*, 72–84. [CrossRef]
17. Wei, Y.; Ma, Y.; Zhang, W. A Multi-Jointed Underactuated Robot Hand with Fluid-Driven Stretchable Tubes. *Robot. Biomim.* **2018**, *5*, 1–10. [CrossRef]
18. Liarokapis, M.; Dollar, A. Post-Contact, In-Hand Object Motion Compensation with Adaptive Hands. *IEEE Trans. Autom. Sci. Eng.* **2018**, *15*, 2. [CrossRef]
19. Steltz, E.; Mozeika, A.; Rembisz, J.; Corson, N.; Jaeger, H. Jamming as an Enabling Technology for Soft Robotics. In Proceedings of the Proc. SPIE7642, Electroactive Polymer Actuators and Devices (EAPAD), San Diego, CA, USA, 8–11 March 2010.
20. Sayyadan, M.; Moniri, M.; Gharib, F. Stiffness Variations in Granular Jamming Robots; an Eperimental Method. In Proceedings of the 22nd International Conference on Methods and Models in Automation and Robotics (MMAR), Międzyzdroje, Poland, 28–31 August 2017.
21. Brown, E.; Rodenberg, N.; Amend, J.; Mozeika, A.; Steltz, E.; Zakin, M.; Lipson, H.; Jaeger, H. Universal Robotic Gripper Based on the Jamming of Granular Material. *Proc. Natl. Acad. Sci. USA* **2010**, *107*, 44. [CrossRef]
22. Amend, J.; Brown, E.; Rodenberg, N.; Jaeger, H.; Lipson, H. A Positive Pressure Universal Gripper Based on the Jamming of Granular Material. *IEEE Trans. Robot.* **2012**, *28*, 341–350. [CrossRef]
23. Shan, Y.; Zhao, Y.; Pei, C.; Yu, H.; Liu, P. A Novel Design of a Passive Variable Stiffness Soft Robotic Gripper. *Bioinspir. Biomim.* **2022**, *17*, 066014. [CrossRef]
24. Cheng, N.; Lobovsky, M.; Keating, S.; Setapen, A.; Gero, K.; Hosoi, A.; Iagnemma, K. Design and Analysis of a Robust, Low-cost, Highly Articulated Manipulator Enabled by Jamming of Granular Media. In Proceedings of the IEEE International Conference on Robotics and Automation, St Paul, MN, USA, 14–18 May 2012.
25. Wei, Y.; Chen, Y.; Yang, Y.; Li, Y. A Soft Robotic Spine with Tunable Stiffness Based on Integrated Ball Joint and Particle Jamming. *Mechatronics* **2016**, *33*, 84–92. [CrossRef]
26. Li, Y.; Wei, Y.; Yang, Y.; Chen, Y. A Novel Versatile Robotic Palm Inspired by Human Hand. *Eng. Res. Express* **2019**, *1*, 015008. [CrossRef]
27. Chopra, S.; Tolley, M.T.; Gravish, N. Granular Jamming Feet Enable Improved Foot-Ground Interactions for Robot Mobility on Deformable Ground. *IEEE Robot. Autom. Lett.* **2020**, *5*, 3975–3981. [CrossRef]
28. Tramsen, H.T.; Heepe, L.; Gorb, S.N. Granular Media Friction Pad for Robot Shoes—Hexagon Patterning Enhances Friction on Wet Surfaces. *Appl. Sci.* **2021**, *11*, 11287. [CrossRef]

29. Jiang, A.; Xynogalas, G.; Dasgupta, P.; Althoefer, K.; Nanayakkara, T. Design of a Variable Stiffness Flexible Manipulator with Composite Granular Jamming and Membrane Coupling. In Proceedings of the IEEE/RSJ International Conference on Intelligent Robots and Systems, Algarve, Portugal, 7–12 October 2012.

30. Jiang, A.; Ranzani, T.; Gerboni, G.; Lekstutyte, L.; Althoefer, K.; Dasgupta, P.; Nanayakkara, T. Robotic Granular Jamming: Does the Membrane Matter? *Soft Robot.* **2014**, *1*, 192–201. [CrossRef]

31. Bakarich, S.E.; Miller, R.; Mrozek, R.A.; O'Neill, M.R.; Slipher, G.A.; Shepherd, R.F. Pump Up the Jam: Granular Media as a Quasi-Hydraulic Fluid for Independent Control Over Isometric and Isotonic Actuation. *Adv. Sci.* **2022**, *9*, 2104402. [CrossRef]

32. McKee, N. Design Optimization of a Variable Stiffness Soft Robotic Gripper Using Finite Element Analysis and Machine Learning. Bachelor's Thesis, Ohio State University, Columbus, OH, USA, 2022.

33. Jiang, A.; Aste, T.; Dasgupta, P.; Althoefer, K.; Nanayakkara, T. Granular Jamming with Hydraulic Control. In Proceedings of the ASME International Design Engineering Technical Conference & Computers and Information in Engineering Conference, (IDETC 2013), Portland, OR, USA, 4–7 August 2013.

34. Jiang, A.; Aste, T.; Dasgupta, P.; Althoefer, K.; Nanayakkara, T. Granular Jamming Transitions for a Robotic Mechanism. In *AIP Conference Proceedings*; American Institute of Physics: College Park, MD, USA, 2013; Volume 1542, p. 385.

35. Al Abeach, L.; Nefti-Meziani, S.; Theodoridis, T.; Davis, S. A variable Stiffness Soft Gripper Using Granular Jamming and Biologically inspired Pneumatic Muscles. *J. Bionic Eng.* **2018**, *15*, 2. [CrossRef]

36. Howard, D.; O'Connor, J.; Brett, J.; Delaney, G.W. Shape, Size, and Fabrication Effects in 3D Printed Granular Jamming Grippers. In Proceedings of the 2021 IEEE 4th International Conference on Soft Robotics (RoboSoft), New Haven, CT, USA, 12–16 April 2021; pp. 458–464.

37. Fitzgerald, S.G.; Delaney, G.W.; Howard, D.; Maire, F. Evolving Soft Robotic Jamming Grippers. In Proceedings of the GECCO'21 (Genetic and Evolutionary Computation Conference), Lille, France, 10–14 July 2021.